Design of fibrous filter media based on the simulation of pore size measures

Jürgen Becker, Andreas Wiegmann and Volker Schulz
Fraunhofer Institut für Techno- und Wirtschaftsmathematik,
Fraunhofer Platz 1, 67663 Kaiserslautern, Germany

ABSTRACT

Filtration media including woven cloths, nonwoven, membranes and particulate beds are used in a wide variety of applications such as biotech, health care, pharmaceutical, food and beverages, power sources and chemical industries. One way to characterise the performance of all these filtration media is by the pore structure characteristics of the media. Several experimental techniques are available to measure such characteristics, each of them producing a different outcome.
Having the aim to find the optimal design of filtration media with numerical simulations, it is necessary to be able to predict the outcome of pore size measurements as this allows a comparison of virtually created filtration media with existing filtration media.
This paper focusses on the numerical simulation of mercury intrusion porosimetry and liquid extrusion porosimetry. First, the numerical method will be introduced and applied on a sample nonwoven. Results of both methods will be presented and related to the real pore structure of the medium.
Afterwards, the influence of a change in a single production parameter on the pore distribution will be investigated exemplarily. Finally - to validate the method – the numerical results will be compared with experimental findings.

KEYWORDS

Filter Media, Simulation, Pore Size Measures

INTRODUCTION

The performance of filtration media is strongly determined by the pore structure of the media. The size distribution of the pores can be measured by different techniques like mercury intrusion porosimetry, liquid extrusion porosimetry and flow porometry [Jen02]. When the same porous media is measured with two different techniques, the outcome of both measurements differ, although both results are in general called 'pore size distribution'. This is due to the fact that certain pore structures contribute differently to the measured result for different experimental setups. Some methods are able to see 'blind' pores and through pores whereas others only capture through pores. Some techniques measure only the most constricted radius of a pore, wheras others can attribute varying radii to one pore. So in general only results obtained with the same measurement technique are comparable.
When designing filtration media on the computer a three dimensional model of the microstructure is generated. This allows to calculate the geometric pore sizes of the media directly. Nevertheless, the resulting pore size distribution is in general not directly comparable with measurements, as it is calculated in a completely different way. Therefore an approach is needed to predict the outcome of the measurements. This can be achieved by adjusting the numerical calculations in such a way, that blind pores, through pores and closed pores contribute to the result as in the experimental measurements. So the result of the new numerical approach is no longer the distribution of the geometric sizes of the pores but the size distribution as the measurement technique would see it, which makes the result comparable to measurements.

SIMULATION OF PORE SIZE MEASUREMENTS

Microstructure Generation

Starting point of the numerical method is the construction of a three dimensional microstructural model of the porous media. Such a model can be obtained either from a tomography image of the filtration media or by creating a three dimensional model virtually. While tomography images can be used to compare measurement and simulation (but might be costly), computer generated models are necessary when designing new filtration media. The virtual reconstruction of the filtration media uses statistical material parameters such as porosity and mean fibre thickness as input and applies methods from statistical geometry to generate a model (see also [Tor02],[Sch05]). Nevertheless, if the generated sample represents a large enough part of the porous media, the results are representative.
Here – as example to demonstrate the numerical methods presented in the following – we generated a nonwoven fibre mat with a size of 512 x 512 x 128 µm and an overall porosity of 82%. The resolution is 1 µm per voxel. The fibres have a circular cross section, a diameter of 7 µm and are oriented along the x-y plane. Figure 1 shows a picture of the created structure.

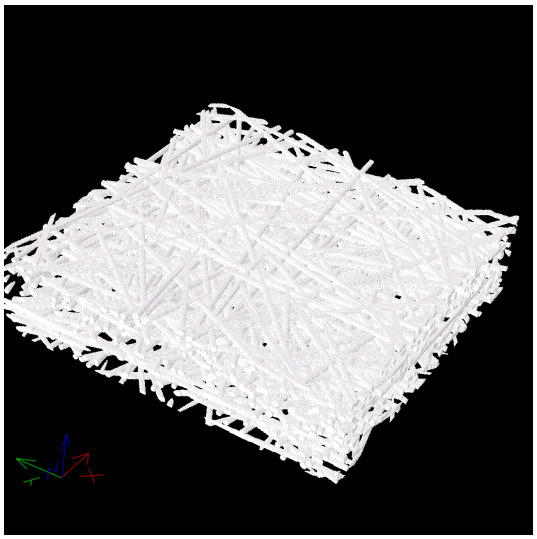

Figure 1: 3d picture of the sample nonwoven used as an example in this chapter's numerical pore size calculations.

Geometric Pore Sizes

Given a three dimensional model of the porous media the size of the pores can be calculated directly from the data. To give the notion of 'pore radius' a meaning also in the case of non-cylindrical pores (compare e.g. figure 1), we determine the morphological opening

$$O_r(X) = \bigcup_{\substack{B_{r,x} \subset X, \\ x \in X}} B_{r,x}\,, \tag{1}$$

where X represents the pore space and $B_{r,x}$ is a sphere with radius r and centre point x. In other words, O_r is that part of the pore space, where the structuring element B_r fits in. So it is sensible to define O_r to be by definition the space of pores with radius r or larger, which makes $|O_r|/|X|$ the cumulative pore volume fraction of all pores with radius $r' \geq r$. By choosing different radii r, the distribution of the pore sizes is determined (see also [Hil01]). This approach corresponds to a sieving process of the pores and is known as granulometry [Soi99].

Algorithmically, the opening is determined as a dilation of the eroded pore space with the same structuring element B_r:

$$O_r(X) = D_r(E_r(X))\,, \tag{2}$$

where the erosion is defined by

$$E_r(X) = \{x : B_{r,x} \subset X\} \tag{3}$$

and the dilation is defined as

$$D_r(X) = \bigcup_{x \in X} B_{r,x}\,. \tag{4}$$

So the eroded pore space is the union of all points that are at least r away from the nearest fibre. Thus the first step reduces to finding the Euclidean distance map, which is solved efficiently using Saito's algorithm [Sai94]. A dilation is equivalent to an erosion of the inverted 3D structure and therefore also the second step is solved efficiently by Saito's algorithm. Figure 2 illustrates this approach by showing the resulting pores in a two dimensional example.

The pore size distribution of the sample shown in figure 1 is plotted in figure 4 amongst others.

However, this calculated pore size distribution cannot be compared to standard experimental measurements of pore size distributions, as here we do not take the connectivity of the pores into account. In particular, this method does not distinguish between closed pores, blind pores and through pores.

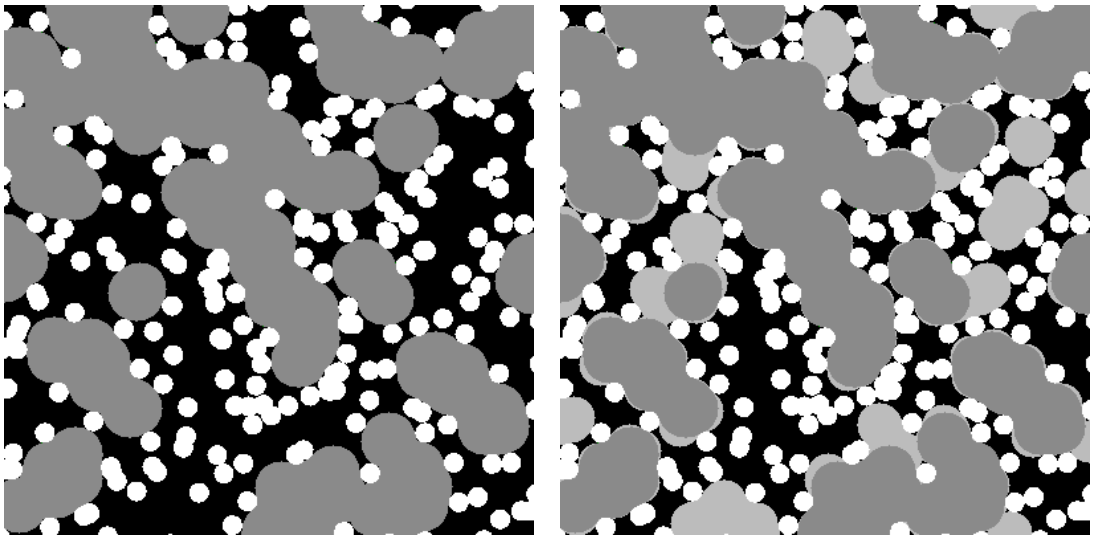

Figure 2: Two dimensional example illustrating the used method of determining pore sizes. The fibres are shown in white, grey areas mark pores of radius $r \geq 20$ and $r \geq 16$, respectively.

Mercury Intrusion Porosimetry

As mercury is non-wetting to most materials, intrusion of mercury into pores only occurs when pressure is applied on the mercury. In the experimental setup, the pressure on the mercury is raised subsequently and the volume of the intruding mercury (which equals the volume of the intruded pores) is measured. The pressure p is related to the pore radius r via the Young-Laplace equation

$$p = \frac{2\gamma}{r}\cos\vartheta, \tag{5}$$

where γ is the surface tension and ϑ the contact angle of mercury. Thus, a size distribution of pores is determined. This method cannot measure the volume of closed pores. In addition, large pores hidden behind smaller bottlenecks are not filled with mercury until the pressure is high enough for the mercury to pass the bottleneck. Therefore, these pores are measured with the size of the bottleneck.

To mimic this experimental setup in the simulation only pores connected to the mercury reservoir must be taken into account. This is achieved algorithmically by first eroding the pore space by r, and then in a second step discarding the parts not connected to the reservoir. In the third step the remaining pore space is dilated by r again. The resulting pore volume is exactly that part of the pore volume reachable by a sphere of radius r flowing in from the reservoir [Hil01].
Figure 3 illustrates this approach by showing the results of the method in a two dimensional example. Here, it was assumed, that the mercury may intrude the nonwoven structure from the top and from the bottom. A comparison of the results shown in figures 2 and 3 shows that the cumulative volume fraction of the pores with

radius $r \geq 20$ or $r \geq 16$ is much lower when measured with mercury intrusion porosimetry.
Simulation results for the sample shown in figure 1 can be found in figure 4.

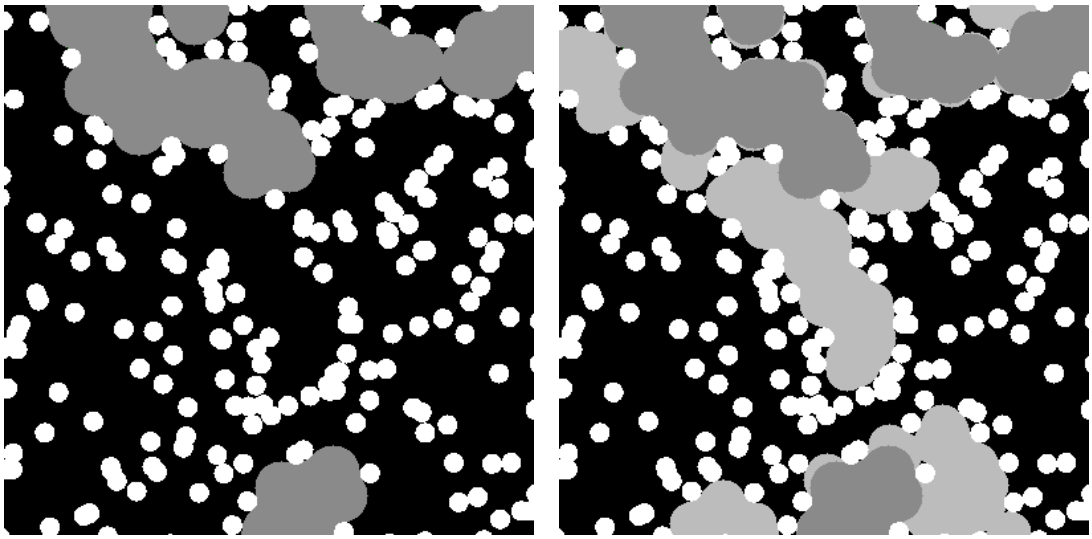

Figure 3: Two dimensional example (same setup as in fig. 2) illustrating the method of a mercury intrusion porosimetry simulation: fibres are plotted white, grey areas mark pores of radius $r \geq 20$ and $r \geq 16$, respectively. All pores marked are always connected to one of the mercury reservoirs on top or bottom of the sample by a wide enough path.

Liquid Extrusion Porosimetry

Here, the pores are initially filled with a wetting liquid and the liquid is then extruded from the pores by a non-reacting gas. To allow the extruded liquid to flow out and to prevent the gas to escape, the sample is placed upon a membrane whose pores are also filled with the wetting liquid. The largest pore of the membrane has to be smaller than the smallest pore of interest in the sample.
The method measures the differential pressure and the volume of the extruding liquid. The differential pressure is again related to the pore radius by the Young-Laplace equation (5), where ϑ and γ denote now contact angle and surface tension of the liquid-gas interface.
Similar to mercury intrusion porosimetry, this method cannot measure the volume of closed pores and produces the same results in the case of bottlenecks. But here, the non-wetting gas intrudes only from one side of the sample. Thus the same approach can be used for the numerical simulation, but with a one-sided reservoir.

The results of the simulation and a comparison with the results of the methods described in the previous paragraphs can be found in figure 4. Compared to mercury intrusion the liquid extrusion exhibits less large pores and the peak is slightly shifted to smaller pore sizes, a fact often observed in the experiment [Jen02]. Both methods tend to underestimate the number of large pores inside the nonwoven mat.

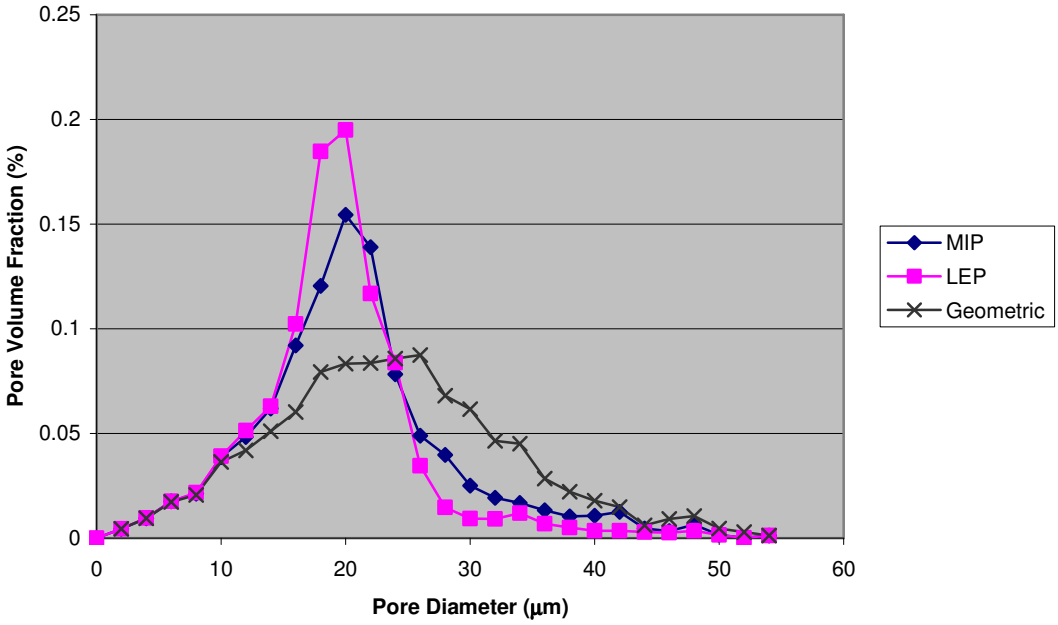

Figure 4: Pore size distribution of the sample shown in figure 1. The diagram shows the calculated geometric pore size distribution and the results of the simulated mercury intrusion (MIP) and the simulated liquid extrusion (LEP).

VIRTUAL DESIGN OF FIBROUS MATERIALS

Nonwoven fibre media are characterised by global production parameters like porosity, fibre length, diameter, cross sectional shape and the (an)isotropic distribution of the fibre orientation. Using virtually generated models, the influence of a single production parameter on the resulting pore size distribution can be examined.

To present this exemplarily, figure 5 shows three pore size distributions for virtually created nonwoven samples with the same fibre type, but different porosities. Here, fibre diameter, length, cross sectional shape and orientation were chosen as in the reference sample shown in figure 1. Unsurprisingly, the sample with the lowest porosity exhibits the smallest pore sizes.
In the same way, the influence of e.g. different cross sectional shapes or fibre radii distributions could be investigated.

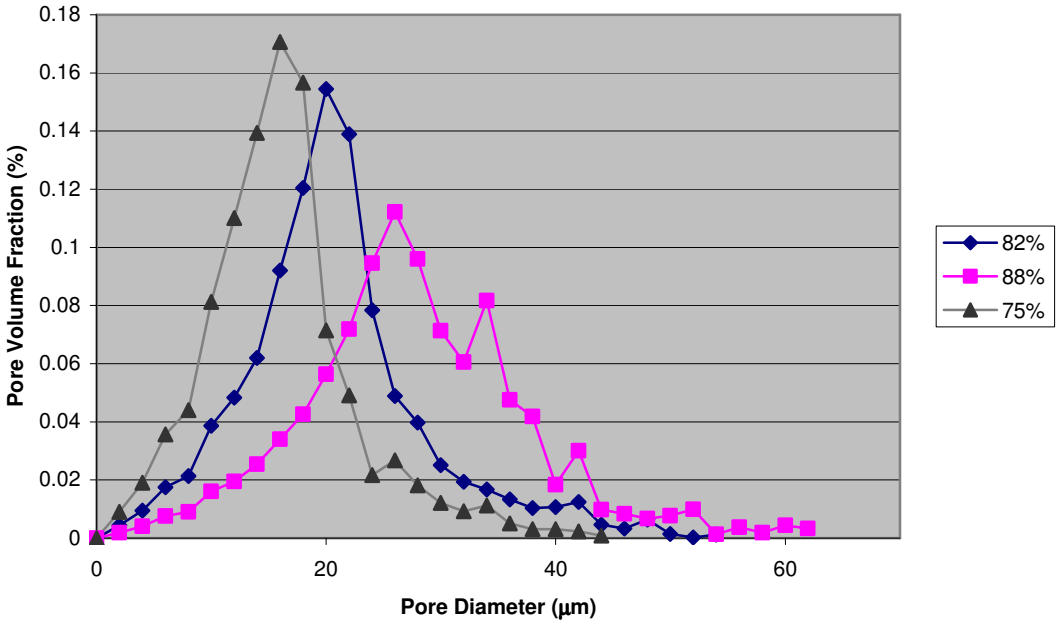

Figure 5: Pore size distribution (simulated MIP) of three nonwoven samples with the same fibre type but with different porosities.

COMPARISON OF MEASUREMENT AND SIMULATION

To be able to compare measurement with simulation a three dimensional model of the filter media under investigation has to be constructed in a first step. Here, a three dimensional model has been generated stochastically taking known material parameters (porosity, fibre size distribution) as input. Figure 6 shows on the right hand side a picture of the generated structure. The resulting pore size distribution plotted in the chart was determined by simulated mercury intrusion porosimetry and is compared to MIP measurements. The peak of the distributions is exactly at the same position (12 µm pore radius) for both curves.

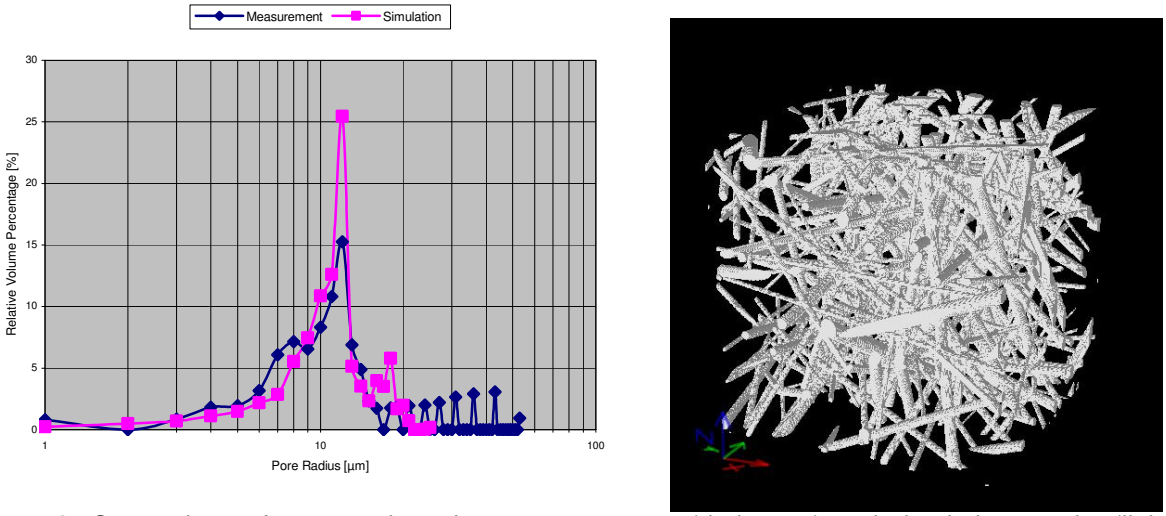

Figure 6: Comparison of mercury intrusion measurements (dark grey) and simulation results (light grey). The picture on the right hand side shows a visualisation of the model used in the simulation.

CONCLUSIONS

With the method presented we are able to predict the outcome of pore size measurements performed by mercury intrusion porosimetry and liquid extrusion porosimetry. This is of great importance when designing filtration media virtually as pore size distributions calculated with the standard 'geometric' approach are in general not comparable with measurements. The examples presented in this paper show that the geometric approach overestimates the amount of large pores when compared to measurements.
In combination with Navier-Stokes simulations the method could also be used to model flow porometry [Jen02] measurements, but this approach would be numerically costly and is not presented here.

REFERENCES

[Hil01] M. Hilpert and C.Miller, *Pore-morphology based simulation of drainage in totally wetting porous media*, Adv. Water Resour., Vol. 24, 2001, pp. 243-255.

[Jen02] A. Jena and K. Gupta, *Characterization of pore structure of filtration media*, Fluid Particle Separation Journal, Vol. 4, No.3, 2002, pp. 227-241.

[Sai94] T. Saito and J.-I. Toriwaki, *New algorithms for Euclidean distance transformations of an n-dimensional digitized picture with applications,* Pattern Recognition, Vol. 27, 1994, pp. 1551-1565.

[Sch05] K. Schladitz, S. Peters, D. Reinel-Bitzer, A. Wiegmann and J. Ohser, *Design of acoutic trim based on geometric modeling and flow simulation for non-woven,* Bericht des Fraunhofer ITWM, Vol. 72, 2005.

[Soi99] P. Soille, *Morphological Image Analysis: Principles and Applications,* Springer, Berlin, 1999

[Tor02] S. Torquato, *Random Heterogeneous Materials,* Springer, New York, 2002.

[Vog05] H.-J. Vogel, J. Tölke, V. Schulz, M. Krafczyk and K. Roth: *Comparison of a Lattice-Boltzmann model, a full-morphology model, and a pore network model for determining capillary pressure-saturation relationships*, Vadose Zone Journal, Vol. 4, 2005, pp. 380-388.